Effect of annealing atmosphere on optic-electric properties of ZnO thin films

C. Bueno[a,*], M. Pacio[b], E. Osorio[c], R. Perez[d], and H. Juarez[b]
[a] *Benemérita Universidad Autónoma de Puebla, Facultad de Ingeniería,*
Blvd. Valsequillo y Av. San Claudio, s/n, San Manuel, 72570, Puebla, México.
[b] *Benemérita Universidad Autónoma de Puebla, Posgrado en Dispositivos Semiconductores, CIDS-ICUAP,*
Blvd. 14 sur y Av. San Claudio, Jardines de San Manuel, 72450, Puebla, México.
**e-mail: cba3009@gmail.com*
[c] *Catedra-Universidad de Quintana Roo,*
Blvd. Bahía s/n, esquina Ignacio Comonfoft, El Bosque, 77019, Chetumal, Quintana Roo.
[d] *Benemérita Universidad Autónoma de Puebla, Facultad de Ingeniería Química,*
Av. Sn. Claudio y 18 sur, Jardines de San Manuel, 72570, Puebla, México.

Received 23 August 2016; accepted 2 August 2017

In this work the study of the structural, morphologic characteristics, optical and electrical properties of the thin films of ZnO in temperatures and annealing atmospheres different was realized. The films were obtained by the sol-gel method, utilizing zinc acetate dihydrate as the precursor, monoethanolamine (MEA) as a stabilizing agent and 2-methoxyethanol as a solvent and deposited by spin-coating. The films were crystallized at 600, 800 and 1000°C in oxygen and nitrogen atmospheres. The results obtained by XRD, SEM, photoluminescence and Hall effects of the ZnO films were related and depend strongly on the temperature and atmosphere annealing.

Keywords: ZnO films; sol-gel; temperature and atmosphere annealing.

PACS: 81.05.Dz; 81.40.-z; 73.61.Ga

1. Introduction

Metal oxide semiconductor films have been widely studied and have received considerable attention in recent years. Particularly ZnO films have great potential applications in light-emitting diodes [1], field-effect transistor [2], flat panel display [3], ultraviolet lasers [4], sensor [5] and solar cells [6], due its properties such as piezoelectric, wide and direct band gap of 3.37 eV and a large exciton binding energy of 60 meV, transparent conductive oxide principally. A lot of methods have been extensively used for oriented ZnO films synthesis, including L-MBE [7], pulsed laser deposition [8], metal-organic chemical vapor deposition [7], cathodic magnetron sputtering [7-10] and reactive electron beam evaporation [11-15], spray pyrolysis [16-19], chemical vapor deposition (CVD) [20], and electrodeposition [21,22]. However, sol-gel processes are particularly adapted to produce ZnO colloids [23] and films [24-25] in a simple, low-cost and highly controlled way. ZnO thin film synthesis by sol-gel method involves several parameters: (1) the nature of the precursor and its concentration, (2) the type of solvent and the acidity of the medium, (3) the type of additive species and their concentrations, (4) the aging time of the early mixture, (5) the method of coating of substrates and its speed, (6) the nature of the substrate, and (7) the pre-heat treatment and temperature annealing of the materials. A survey of the literature shows that all these parameters play a key role on the evolution of texture in zinc oxide film, however, the temperature annealing affects overall film quality, and therefore, the temperature annealing should be carefully chosen. Several authors mention that, the temperature range 500-700°C seems to be the most appropriate [26,32]. So it is difficult to find reports of heat treatment in the range of 600-1000°C in oxygen and nitrogen atmospheres.

The main objective of this work is to study the change in the structural characteristics, optical and electrical properties of ZnO films deposited by the sol-gel method and crystallized at 600, 800 and 1000°C in N_2 and O_2 atmospheres, temperature range employed in the based devices ZnO.

2. Material and methods

ZnO thin films were prepared using the sol-gel method, a solution was synthesized by dissolving zinc acetate dehydrate in 2-methoxyethano (2-ME), and then a stabilizer of monoethanolmine (MEA) was added to the blended solution. The molar concentration of zinc ions was 0.5 M, and the molar ration of MEA to zinc ions was maintained at 1:1. The solution was stirred for 30 min to yield a clear and transparent. All ZnO sol-gel films were spin-coated onto pre-cleaned silicon substrates at a rotations speed of 3000 rpm for 30 s. Each such coated film was heated at 300°C for 15 min to evaporate the solvent, water, and organics. The spin coating and drying procedures above described, were repeated ten times. Finally to achieve crystalline, ZnO films were annealed at 600, 800 and 1000°C for 2 hours in N_2 and O_2 atmospheres. The morphologic of ZnO films was examined by an X-ray diffractometer (Discover D8) with Cu-kα radiation ($\lambda = 1.5406$ Å). The surface morphology of the films was examined using a scanning electron microscope (SEM) Au-

riga de ZEISS model. To investigate the optical property of ZnO films, PL measurement was performed by a fluorescence spectrophotometer Varian, Cary Eclipse model. For electrical properties of ZnO films, the Van der Pauw Hall method was used along with the Hall effects measurement (model Ecopia HMS-5000).

3. Results and discussion

Following the sol-gel coating process, an XRD analysis was performed to investigate the effect of different atmospheres and temperatures annealing on the crystal structure of ZnO films. Figure 1 shows the XRD pattern of ZnO films growth on the silicon substrates annealed in an atmosphere of oxygen (O_2) and nitrogen (N2) at temperatures of 600, 800 and 1000°C. The XRD pattern shows there is a preferential orientation in the plane (002), with type hexagonal wurtzite structure of ZnO, in all cases; however, for the samples annealed at 600°C patterns show also preferential orientations of (100) and (101), this is due to a lower crystallinity with respect to films annealed at 800 and 1000°C. In ZnO films with heat treatment in O_2 atmosphere, it is observed that the crystallinity is increased with temperature [33]. In the case of films annealed in N_2 atmosphere the behavior is similar, except for the samples annealed at 1000°C for which intensity is diminished. Also, it was found that the intensity of (002) diffraction peak increases and the full width at half maximum (FWHM) becomes narrow with temperature and atmospheres annealing. The increase of diffraction intensity and narrowing of FWHW are related to the enhanced crystallinity and increased grain size. The grain size (D) was computed according to the Scherrer [34] Eq. $D = 0.9\lambda/(B\cos\theta)$, were λ, B, and θ are X-ray wavelength (0.15406 nm), FWHW of (002) peak and Bragg diffraction angle, respectively. It was found that the grain sizes were increasing in annealing temperature of 600 to 800°C in both annealing atmospheres, improving the crystallinity. This behavior is related with the decrease the full width at half maximum, and could be relates an inhomogeneous distribution of crystal size, which induces different distances between the planes for the same crystal [35], and the average width increases. The grain sizes for the films annealed in atmosphere of O_2 were 34.6, 71.3 and 68.7 nm for the films annealed in temperature at 600, 800 and 1000°C, respectively. The grain size for the films annealed in atmosphere of N_2 was 30.5, 59.4 and 42.4 nm for the films annealed at 600, 800 and 1000°C, respectively. Figure 2 shows the SEM images of surface the ZnO films obtained at different annealing temperatures. ZnO films annealed at atmosphere 600°C in N_2 and O_2 (Fig. 2a, 2b), the samples have a rough surface, formed by small particles of ZnO. The inset shows these particles are uniformly distributed on the surface of the sample. In case of the ZnO films with annealing at 800°C in N_2 and O_2 atmospheres (Fig. 2c and 2d), the size of this ZnO particles, is greater than films annealed at 600°C and also the ZnO particles cover homogeneous the substrate. The same behavior shown in the ZnO films annealing at 1000°C, the particles size are increased, however the particles size are different (Fig. inset in 2e). Finally, in the case of the film annealed in N_2 atmosphere at 1000°C, the superficial morphology clearly altered probably due to desorption of O_2 at this annealing temperature.

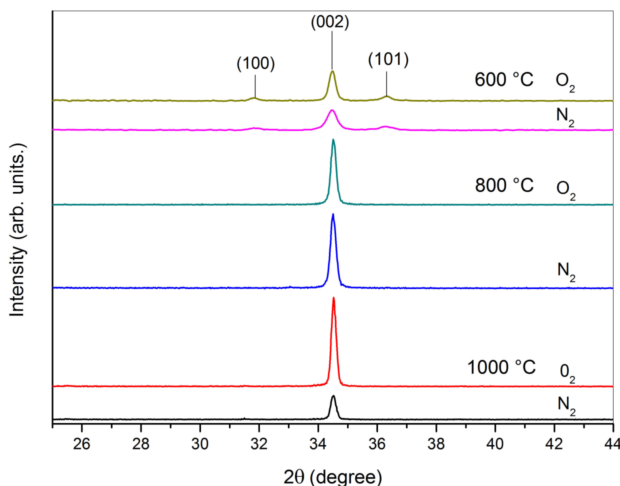

FIGURE 1. XRD patterns of ZnO films annealing in O_2 and N_2 at different temperatures.

A study of the photoluminescence property of ZnO films is very important because it can provide more valuable information on the quality and purity of the material. Figure 3 shows the PL spectra of annealed ZnO films. Two UV emission peak centered at 362 and 380 nm, and a weak blue emission at 405 nm were obtained for all the ZnO film. The strong and sharp emission in 382 nm corresponds to the transition from free exciton (FX). The intensity of this emission is related to ZnO films with higher quality crystalline [36], this corresponds to the films annealed in O_2 atmosphere at 800 and 1000°C and in N_2 atmosphere at 800°C. The emission band centered at 362 nm is excitonic nature regarding donor or acceptor levels [37]. Finally, the emission at 405 nm (3.14 eV) is attributed to transitions related acceptor levels due to zinc vacancies, VZn or excess de oxygen, [38]. As seen in the case of annealing O_2 at 1000°C.

Figure 4 shows the results of the Hall Effect measurements at 300 K, carrier concentration versus annealing temperature for two annealing atmosphere (Fig. 4a). Fig. 4a shows that 600°C annealing temperature versus the carrier concentration. In this graph shown, when the annealing temperature is 600°C has a higher carrier concentration for both atmospheres. This is related to the crystalline quality of the films and the grain size these are similar for two atmospheres annealing, and thus the intrinsic defects in the films are similar, and these values of n corresponds to a semiconductor degenerate [39,40]. When the temperature annealing increased to 800°C, carrier concentration decreases with respect at the annealed films at 600°C at both annealing atmospheres, this result could be associated with higher peak intensity X-ray diffraction of the plane (002) [35], *i.e.*, if the carrier concentration decreases, probably the tension on the lattice decrease

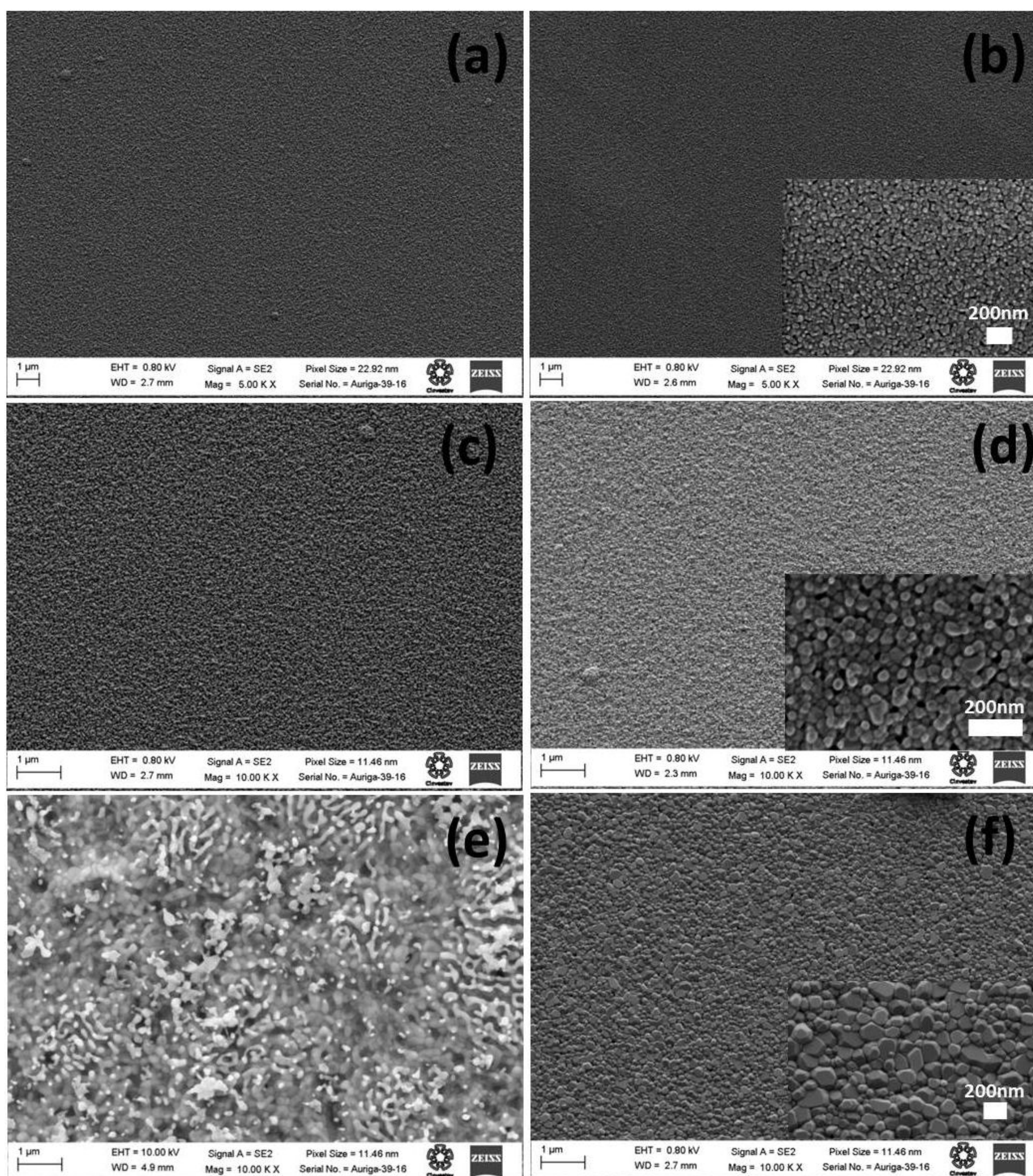

FIGURA 2. Surface morphologic of the ZnO films deposited by sol gel method, the atmosphere annealing N_2 (right), O_2 (left) and annealing temperatures of (a,b) 600, (c,d) 800 and (e,f) 1000°C

and thereby improves the crystalline quality of the films. The value of the carrier concentration for annealing in N_2 is greater this is due to desorption of O_2, increasing the vacancies of O_2 and therefore the value carrier concentration incremented [38]. For the annealing temperature of 1000°C, the value of the carrier concentration was increased for the annealing atmosphere at N_2 due to increased of vacancies of O_2, however for annealing atmosphere at O_2 the value of the carrier concentration remains as the film annealed at 800°C. This result be associated with the spectra of X-ray diffraction, which showed that the crystalline quality decreases with annealing atmosphere at N_2 and for the O_2 is similar (in peak intensity and width FWHM). Figure 4b shows the mobility versus the temperature and atmosphere annealing. Shows that annealing temperature 600°C is low and mobility similar value for both annealing atmospheres, this due to the high concentration of carriers, so that there is a high dispersion of the evaporators for defects. When the annealing temperature was 800°C mobility increases according to the decrease in carrier concentration, being higher for films with the annealing atmosphere O_2 in N_2. Finally, to the annealing temperature of 1000°C is observed that decreases mobility for

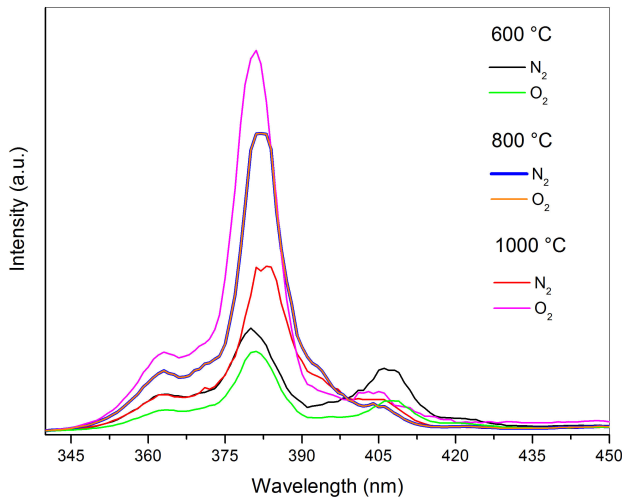

FIGURE 3. RT PL spectrum of ZnO films at different temperatures and atmospheres annealing.

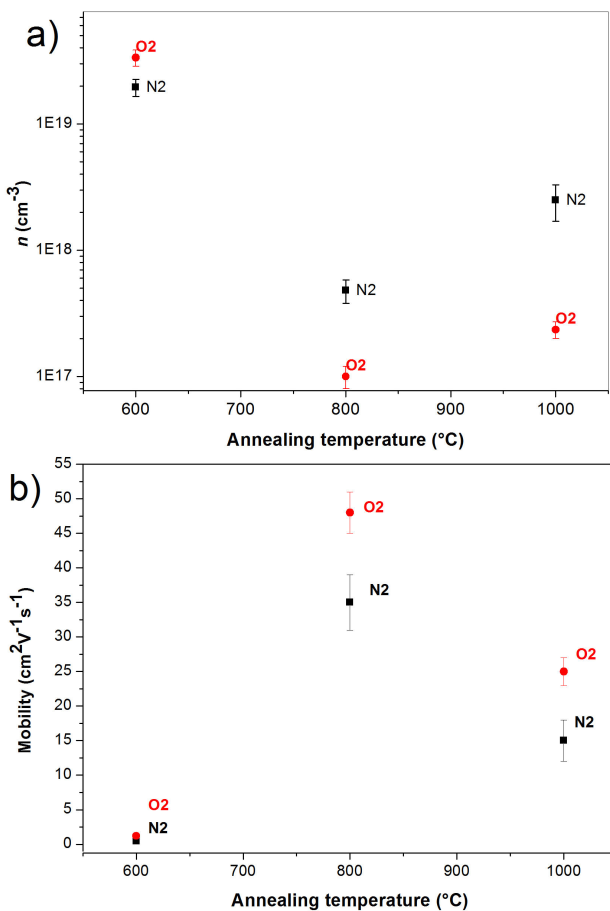

FIGURE 4. Carrier concentration (a) and mobility (b) of the ZnO films versus temperature and atmospheres annealing.

samples annealed at 800°C, again due to increased carrier concentration, even though the films are annealed at 1000°C less grain boundaries, as shown in Fig. 2 based on this result we can say that the dominant mechanism of scattering of carriers is due to defects not electrically activated and grain boundary scattering.

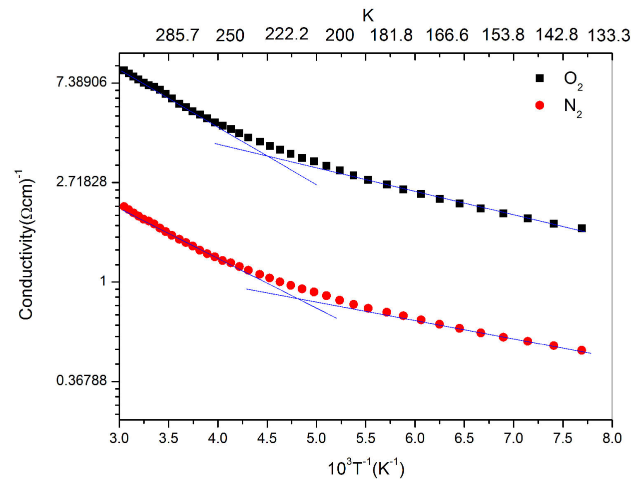

FIGURE 5. Conductivity versus $1/T$ of the ZnO films

TABLE I. Values obtained donor level of ZnO thin films.

Annealing	E_{d1}(eV)	E_{d2} (eV)
O_2	0.216	0.438
N_2	0.220	0.420

The conductivity versus 1/T characteristics of typical ZnO films in N_2 and O_2 annealing atmosphere are shown in Fig. 5. At temperatures values above 220 K, there are two possible transport carriers mechanisms, the thermally excited carriers from the conduction band from the donor levels and the carrier transport by thermionic emission due the grain boundaries [41]. For this temperature range, can coexist two transport mechanisms; however the dominant mechanism corresponds to the first mentioned above, because the emission via grain boundaries was not adequate. At temperatures below 220 K, various authors mention that the transport mechanism may be due to conduction through neighboring donor levels, however, there is no accordance in the literature Y. Natsume *et. al.* [41] mentioned that can be obtained for values less than 200 K, P. Sagar *et. al.* [39] suggests that this mechanism should occur at temperatures below 100 K. In this work the dependence of the conductivity as a function is according to $T^{-1/4}$. Thus, the transport mechanism dominant could correspond to carrier transport through the conduction band from thermally excited donor levels, so that we can use the following expression:

$$\sigma = \sigma_1 \exp\left(\frac{-E_{a1}}{kT}\right) + \sigma_2 \exp\left(\frac{-E_{a2}}{kT}\right) \quad (1)$$

E_{a1} and E_{a2} which correspond to the activation energies of donor levels, k the Boltzmann constant and σ_1, σ_2 pre-exponential factors. In Fig. 3.10, shows the slopes were the activation energy and the donor levels was obtained with respect to the conduction band (the donor level values are obtained from the relationship $E_{d1} = 2E_{a1}$ and $E_{d2} = 2E_{a2}$).

Values obtained donor level (Table I) are similar to the results from films annealed at atmosphere of N_2 and O_2, according to the literature this corresponds to the presence of native defects such as zinc interstitial and oxygen vacancies or both [42]. Similar values were obtained by several authors [43-46].

4. Conclusions

In this work is shown that the structural optical and electrical properties are dependent to the temperature and the annealing atmospheres for the films obtained by this method. According to the XRD patterns the thin films shows 002 preferential orientation, where the intensity of the peak increases with the temperature except for the film annealing at 1000°C in atmosphere of N_2 due of the desorption of O_2.

The results show that the thin films exhibit a major cristallinity quality and have a high emission at UV band at room temperature and a weak emission in the visible region.

From the results obtained in the electrical characterization shows that the carrier concentration and the mobility depend directly of the temperature and annealing atmosphere. However the increasing of the annealing temperature causes the decreasing of the carrier concentration therefore the rise of the mobility. In this work the increase of the mobility depend directly to the values lower of the carrier concentration and the mechanism of the dispersion dominant are just by defects and not by the grain boundaries.

1. X.S. Nguyen, C.B. Tay, E.A. Fitzgerald, and S.J. Chua, *small* **8** (2012) 1204.
2. Z.Y. Fan, and J.G. Lu, *Appl. Phys. Lett.* **86** (2005) 32111.
3. M.C. Elvira *et al*., *Appl. Phys. Lett.* **85** (2004) 2541.
4. J.Y. Kim, H. Jeong, and D.J. Jang, *J. Nanopart. Res.* **13** (2011) 6699.
5. D. Berger *et al*., *Ceramics International* **42** (2016) 13555-13561.
6. A.J. Gimenez, J.M. Yáñez-Limón, and J.M. Seminario, *J. Phys. Chem. C* **115** (2011) 282.
7. A. Tsukazaki *et al*., *Nature Materials* **4** (2005) 42-46.
8. S.V. Prasad, S.D. Walck, and J.S. Zabinski, *Thin Solid Films* **360** (2000) 107.
9. D.K. Hwang, K.H. Bang, and M.C. Jeong, J.M.M. Young, *J. Cryst. Growth* **254** (2003) 449.
10. L.Y. Lin, M.C. Jeong, D.E. Kim, and J.M. Myoung, *Surf. Coat. Technol* **201** (2006) 2547.
11. M. Martin, M.-S. Good, J.-W. Johnston, G.-J. Posakony, L.-J. Bond, and S.-L. Crawford, *Thin Solid Films* **379** (2000) 253.
12. R. Ondo-Ndong, F. Delannoy, A. Giani, A. Boyer, and A. Foucaran, *Mater. Sci. Eng. B* **97** (2003) 68.
13. R. Ondo-Ndong, G. Ferblantier, M. Al Khalfioui, A. Boyer, and A. Foucaran, *J. Cryst. Growth* **255** (2003) 130.
14. R. Al Asmar, G. Ferblantier, F. Mailly, and A. Foucaran, *Phys. Status Solidi C* **2** (2005) 1331.
15. R. Al Asmar, G. Ferblantier, F. Mailly, P. Gall-Borrut, and A. Foucaran, *Thin Solid Films* **473** (2005) 49.
16. R. Romero, D. Leinen, E.-A. Dalchiele, J.-R. Ramos-Barrado, and F. Martín, *Thin Solid Films* **515** (2006) 1942.
17. S.M. Abrarov, Sh.U. Yuldashev, T.W. Kim, S.B. Lee, H.Y. Kwon, and T.W. Kang, *J. Lumin.* **114** (2005) 118.
18. S.M. Abrarov *et al*., *Opt. Commun.* **250** (2005) 111.
19. R. Ayouchi *et al*., *Thin Solid Films* **426** (2003) 68.
20. H. Deng, J.J. Russell, R.N. Lamb, B. Jiang, Y. Li, and X.Y. Zhou, *Thin Solid Films* **458** (2004) 43.
21. T. Pauporte*i*, and D. Lincot, *Electrochim. Acta* **45** (2000) 3345.
22. E.-B. Yousfi, J. Fouache, and D. Lincot, *Appl. Surf. Sci.* **153** (2000) 223.
23. Z. Hu, G. Oskam, and P.C. Searson, *J. Colloid Interface Sci.* **263** (2003) p. 454.
24. Amanpal Singh, Dinesh Kumar, and P.K. Khanna, MukeshKumar, *Materials Letters* **183** (2016) 365-368.
25. Lamia Znaidi, *Materials Science and Engineering B* **174** (2010) 18.
26. Amanpal Singh, Dinesh Kumar, P.K.Khanna, and MukeshKumar, *Materials Letters* **183** (2016) 365-368
27. P.T. Hsieh, Y.C. Chen, K.S. Kao, M.S. Lee, and C.C. Cheng, *J. Eur. Ceram. Soc.* **27** (2007) 3815.
28. P.T. Hsieh, Y.C. Chen, M.S. Lee, K.S. Kao, M.C. Kao, and M.P. Houng, *J. Sol-Gel Sci. Technol.* **47** (2008) 1.
29. S.H. Yoon, D. Liu, D. Shen, M. Park, and D.J. Kim, *J. Mater. Sci.* **43** (2008) 6177.
30. G. Srinivasan, N. Gopalakrishnan, Y.S. Yu, R. Kesavamoorthy, and J. Kumar, *Super-lattices Microstruct.* **43** (2008) 112.
31. G. Srinivasan, R.T. Rajendra Kumar, and J. Kumar, *J. Sol-Gel Sci. Technol.* **43** (2007) 171.
32. Lamia Znaidi, *Materials Science and Engineering B.* **174** (2010) 18.
33. ShenghongYeng, Ying Liu, Yueli Zhang and Dang Mo, and Bull, *Mater. Sci.* **33** (2010) 209.
34. Amanpal Singh, Dinesh Kumar, P.K. Khanna, Mukesh Kumar, and B. Prasad, *J. Mater. Sci: Mater Electron* **24** (2013) 4607-4613.
35. Xu Jiang-ping, Shishao-bo, Li Lan, Zhang Xiao-Song, Wang Ya-Xin, and Chen Xi-Ming *Chin. Phys. Lett*. **27** (2010).
36. Yuantao Zhang, Guotong Du, Baolin Zhang, Yongguo Cui, HuichaoZhu and Yuchun Chang, *Semicond. Sci. Technol.* **20** (2005) 1132.
37. M. Pan, J. Nause, V. Rengarajan, R. Rondon, E.H. Park, and I.T. Ferguson, *Journal of Electronic Materials* **36** (2007) 457.

38. B. Lin, Z. Fu, and Y. Jia, *Applied Physics Letters* **79** (2001) 943-945.
39. P. Sagar, M. Kumar, and R.M. Mehra, *Materials Science-Poland* (2005) p.23.
40. M. Bouderbala, S. Hamzaoui, M. Adnane, T. Sahraoui and M. Zerdali, *Thin Solid Films* **517** (2009) 15876.
41. Y. Natsume and H. Sakata, *Thin Solid Films* **372** (2000) 30.
42. M. de la L. Olvera, A. Maldonado, R. Asomoza, M. Konagai, and M. Asomoza, *Thin Solid Films* **229** (1993) 196.
43. Zilan Wang, S.C. Su, M. Younas, F.C.C. Ling, W. Anwandb, and A. Wagner, *RSC Adv.* **5** (2015) 12530-12535.
44. Hong Seong Kang, Jeong Seok Kang, Jae Won Kim, and Sang Yeol Lee, *J. Appl. Phys.* **95** (2004) 2146-1250.
45. P. Mitra, A.P. Chatterjee, and H.S. Maiti, *Materials Letters* **35** (1998) 33-38.
46. Peiliang Chen, Xiangyang Ma, and Deren Yang, *J. Appl. Phys.* **101** (2007) 053103.